Numerical simulation of drop array impingement onto a superheated wall

Henrik Sontheimer*, Johannes Kind, Peter Stephan, and Tatiana Gambaryan-Roisman

Institute for Technical Thermodynamics, Technical University of Darmstadt,
Peter-Grünberg-Straße 10, 64287 Darmstadt, Germany

Abstract

Spray cooling is a very efficient method for thermal management of high-performance electronics. The performance of spray cooling is determined by the fluid dynamics and the heat transport when a single drop or multiple drops hit the superheated wall. To understand this process, we numerically study the generic situation of simultaneous impingement of periodic drop arrays onto a superheated wall. We study three different cases in which the distance between the drops varies. The refrigerant used is perfluorohexane (FC-72) in a pure vapor atmosphere under saturation conditions. Drops impinge at moderate Reynolds and Weber numbers, where no splashing occurs during single drop impingement. The wall temperature is above the saturation temperature of the fluid but below the onset of nucleate boiling. Simulations are performed using the OpenFOAM software library, taking into account a dynamic contact angle, evaporation and conjugate heat transfer. We show that the coalescence of more than two drops results in the formation of a liquid jet. A small distance between the drops results in the formation of a thin liquid film while a large distance results in small drops sitting on the wall. In the latter case, the largest amount of heat is transferred, but the occurrence of dry spots is undesirable for cooling applications. The results contribute to a better understanding of spray cooling and provide a perspective for efficient spray cooling.

Keywords

drop array impingement, heat transfer, evaporation, numerical simulation

Introduction

One of the most suitable methods for removing large amounts of heat from high-end electronic devices is spray cooling. It is characterized by a uniform surface temperature and low fluid consumption [1]. However, the fluid dynamics and heat transport phenomena in the spray are very complex and not yet fully understood [2-4]. To break down the complexity of the system, several studies have been conducted to analyze experimentally, numerically, and theoretically a single drop impinging a wall [5-10]. These studies provide essential insight into the fundamentals of fluid dynamics and heat transfer, which are crucial for understanding spray cooling processes.

However, the spray cooling process cannot be treated as a simple superposition of multiple single drop impingement scenarios. As complexity increases, studies examining successive drops, drop trains, and both simultaneous and non-simultaneous drop impingement of two drops aim to bridge the gap between the single drop impingement and the more complex dynamics of spray impacts. There are a few experimental and numerical studies focusing on simultaneous impingement of two drops onto a superheated wall [4]. However, the presence of more than two drops changes the fluid dynamics and heat transport. The simultaneous impingement of more than two drops is referred to as the drop array impingement. This scenario is studied numerically in this work.

In the case of the simultaneous impingement of two drops on a wall, an uprising liquid sheet at the intersection of the two coalescing drops can occur. This uprising liquid sheet has a semi-lunar shape. Its height is greatest in the center of the intersection line, where high velocities perpendicular to the intersection line are observed [11,12]. With increasing kinetic energy, the height and width of this liquid sheet increases. High kinetic energy is observed because of a low horizontal distance between the two drops [11,13-16] or high impact velocities [13,15]. The horizontal distance between the drops is usually described by the spacing parameter

$$e = \frac{d}{D_0}, \tag{1}$$

where d and D_0 denote horizontal distance between the drops and initial drop diameter, respectively. Finally, the liquid sheet collapses. This enhances the mixing of the two drops [12].

In general, the coalescence of two drops results in a smaller wetted area and a lower heat transfer compared to two non-interacting drops impinging a superheated wall [13,14,17]. It is observed that the heat transfer decreases with decreasing spacing [14,18] and decreasing impact velocity [18]. Similar to the case of the single drop impingement, increasing the wall superheat decreases the wetted area [14,15] and increases the heat transfer [14,17]. The non-interacting part of the rim of the spreading drop behaves similar to the case of the single drop impingement [14]. This is, however, not the case during the drop array impingement.

To the best of our knowledge, the work [16] is the only one that investigates the drop array impingement onto a dry wall. This numerical work shows that the impingement regime might change due to the presence of more than two drops. For a small spacing, the periodic square drop array impingement results in splashing and bouncing phenomena that are not observed for the impingement of three drops in a line with identical impact parameters. Splashing and bouncing phenomena are the result of a high rate of conversion of surface energy into kinetic energy. On the other hand, for a larger spacing, the drop array impingement results in the same impingement regime as the drop line impingement. However, instead of a sessile drop, a thin liquid film covering the wall is finally formed.

To the best of our knowledge, there is no work that focuses on the drop array impingement onto a superheated wall. The results reported in the literature show that the fluid dynamics can change drastically compared to two simultaneously impinging drops. Therefore, we expect corresponding significant changes in heat transfer. To quantify these changes, we study numerically the impingement of a drop array onto a superheated wall. The impact parameters are chosen such that a single drop impingement would result in the drop deposition regime. The wall superheat is low, i.e. below the onset of nucleate boiling. We vary the drop spacing and compare the drop array impingement with two simultaneously impinging drops with the same impingement parameters. This work contributes to the understanding of the fluid dynamics and heat transport during drop impingement. From this, recommendations for efficient spray cooling can be derived.

Simulation setup

Our numerical solver is based on the *multiRegionPhaseChangeFlow* solver from the TwoPhaseFlow library [19] within the OpenFOAM framework. A comprehensive description of the solver is given in [20]. In contrast to the original solver, we have improved the modelling of conjugate heat transfer and included a dynamic contact angle model.

The computational domain is divided into two regions: solid and fluid. In the solid region, the transient heat conduction equation is solved:

$$\frac{\partial(\rho_s h_s)}{\partial t} = \nabla\left(\frac{\lambda_s}{c_{p,s}}\nabla h_s\right). \quad (2)$$

In the fluid region, the interface is tracked using the Volume-of-Fluid method. The volume fraction is introduced as the ratio of the liquid volume within the cell to the cell volume. The conservation equation for the volume fraction is given by

$$\frac{\partial(\alpha)}{\partial t} + \nabla\cdot(\boldsymbol{u}\alpha) = \dot{\alpha}_{\mathrm{pc}}. \quad (3)$$

The plic-RDF [21] and isoAdvector [22] approach are used to reconstruct and advect the liquid-vapor interface.

In addition, the conservation equations for mass, momentum and energy are solved:

$$\nabla\cdot\boldsymbol{u} = \frac{\dot{\rho}_{\mathrm{pc}}}{\rho}, \quad (4)$$

$$\rho\left(\frac{\partial\boldsymbol{u}}{\partial t} + (\boldsymbol{u}\cdot\nabla)\boldsymbol{u}\right) = -\nabla p_{\mathrm{rgh}} + \mu\nabla^2\boldsymbol{u} + \boldsymbol{f}_g + \boldsymbol{f}_{\boldsymbol{\sigma}}, \quad (5)$$

$$\frac{\partial(\alpha_i\rho_i c_{p,i}T_i)}{\partial t} + \nabla\cdot\left(\alpha_i\rho_i c_{p,i}T_i\boldsymbol{u}\right) = \alpha_i\nabla^2 T_i + \dot{q}_{\mathrm{pc}}. \quad (6)$$

The energy equation is formulated using a two-field approach, where *i* describes liquid or vapor. The source terms in the momentum equation describe the influence of gravity and surface tension forces. The source terms in the mass and energy equation account for phase change. The evaporation model uses the implicit, gradient-based formulation from [18]. To enhance numerical stability, the mass source terms are smeared according to the method described in [23].

Usually, for multiphase flow simulations, the averaging approach of the Volume-of-Fluid method results not in the physically correct heat flux maximum at the contact line. To overcome this issue, we assume that in fluid cells adjacent to the wall containing both liquid and vapor only the liquid is in contact with the wall. Moreover, for cells containing both liquid and vapor, the conjugate heat transfer is only calculated between the adjacent solid cell and the liquid portion of the fluid cell. From this, the heat flux is evaluated using the corresponding temperature gradients. In cells containing the contact line, significant phenomena occur on a length scale much smaller than the cell size. However, these phenomena can be described by the micro region model based on [24] and described in detail in [18,25]. We include this micro region model as a sub-grid model for all contact line cells. In cells containing the contact line, an additional heat flux is imposed resulting from the micro region model. We use the same sub-grid model to determine the dynamic contact angle as a function of wall superheat and contact line velocity. In order to speed up the computations, correlations are derived from the results of the sub-grid model.

We choose the time step criterion similar to [26], which considers both convective and capillary criteria. The numerical grid is a static, hexahedral mesh. It is refined several times in the regions of interests resulting in a smallest cell size of $\Delta x = 4\mu\mathrm{m}$.

As it is shown in Fig. 1, we use four symmetry planes and simulate four quarter drops. All initial parameters are chosen similar to corresponding experiments [14] on the horizontal coalescence of two drops. The working fluid used is perfluorohexane (FC-72) at saturation conditions ($p_{\mathrm{sat}} = 0.91\,\mathrm{bar}$, $T_{\mathrm{sat}} = 327.15\,\mathrm{K}$). Initial drop diameter, impact velocity and wall superheat are $D_0 = 0.93\mathrm{mm}$, $u_0 = 0.53\mathrm{m\,s^{-1}}$ and $\Delta T = 7.3\mathrm{K}$, respectively. The wall (calcium fluoride: $\rho_s = 3180\,\mathrm{kg\,m^{-3}}$, $c_{p,s} = 854\,\mathrm{J\,kg^{-1}\,K^{-1}}$, $\lambda_s = 9.71\,\mathrm{W\,m^{-1}\,K^{-1}}$) is heated with a heat flux of $\dot{q}_{\mathrm{heater}} = 2150\mathrm{Wm^{-2}}$ in the solid cells adjacent to the fluid. The corresponding Reynolds, Weber, Bond and Jakob number are $Re = 1775$, $We = 48.8$, $Bo = 0.4$ and $Ja = 0.09$, respectively. The spacing parameters are $e = 1.18$, $e = 2.15$ and $e = 3.33$.

A validation of the numerical model is given in [20-22]. In addition, we use the case of the single drop impingement onto a superheated wall and compare the numerical predictions with corresponding experiments [26]. In Fig. 2, the temporal evolution of the wetted area and the heat flow from the wall to the drop are shown, respectively. Quantitatively, the numerical predications agree very well with the experimental data. However, the numerical model predicts a slightly larger maximal wetted area. The receding velocity is predicted accurately. The oscillations in the sessile drop phase are slightly less pronounced in the numerical results compared to the experiments. From this follows a larger heat flow in the simulations compared to the experiments. The occurrence of the much higher predicted maximal heat flow is a result of a much higher temporal and spatial resolution in the simulations compared to the experiments. More details regarding this offset are discussed in [26].

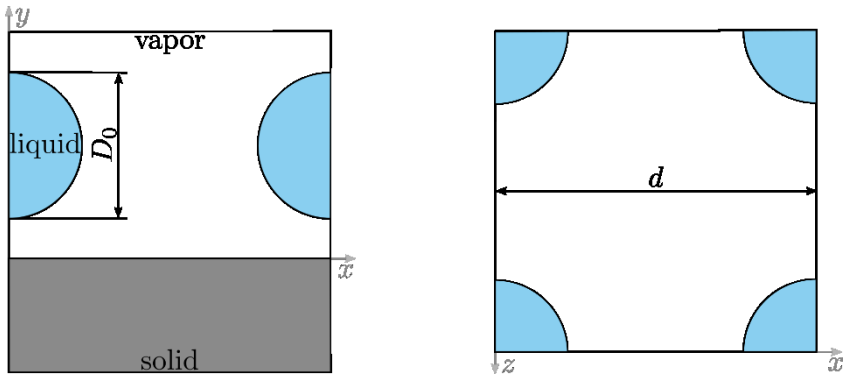

Figure 1 Computational domain for the drop array impingement, side view (left) and top view (right).

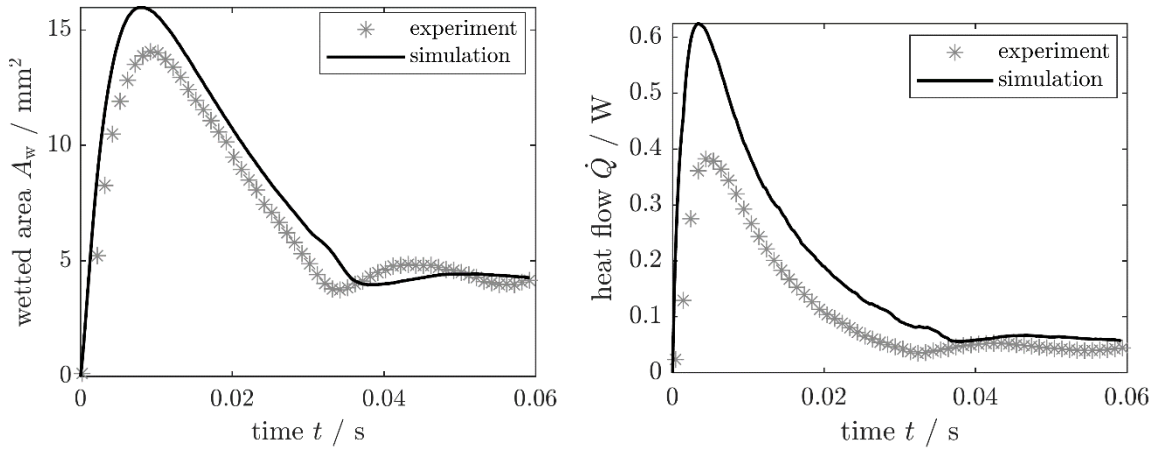

Figure 2 Comparison of the numerical simulation with corresponding experiments [26] for the case of the single drop impingement: temporal evolution of the wetted area (left) and heat flow from the wall to the drop (right).

Results and Discussions

The temporal evolution of the wall temperature and the liquid-vapor interface for three different spacing parameters of the drop array impingement are shown in Fig. 3. Just after the drops hit the wall, the drops spread similar to the case of the single drop impingement (see $t = 0.0002$ s). For a small spacing, i.e. $e = 1.18$, the drops have still very high kinetic energy when

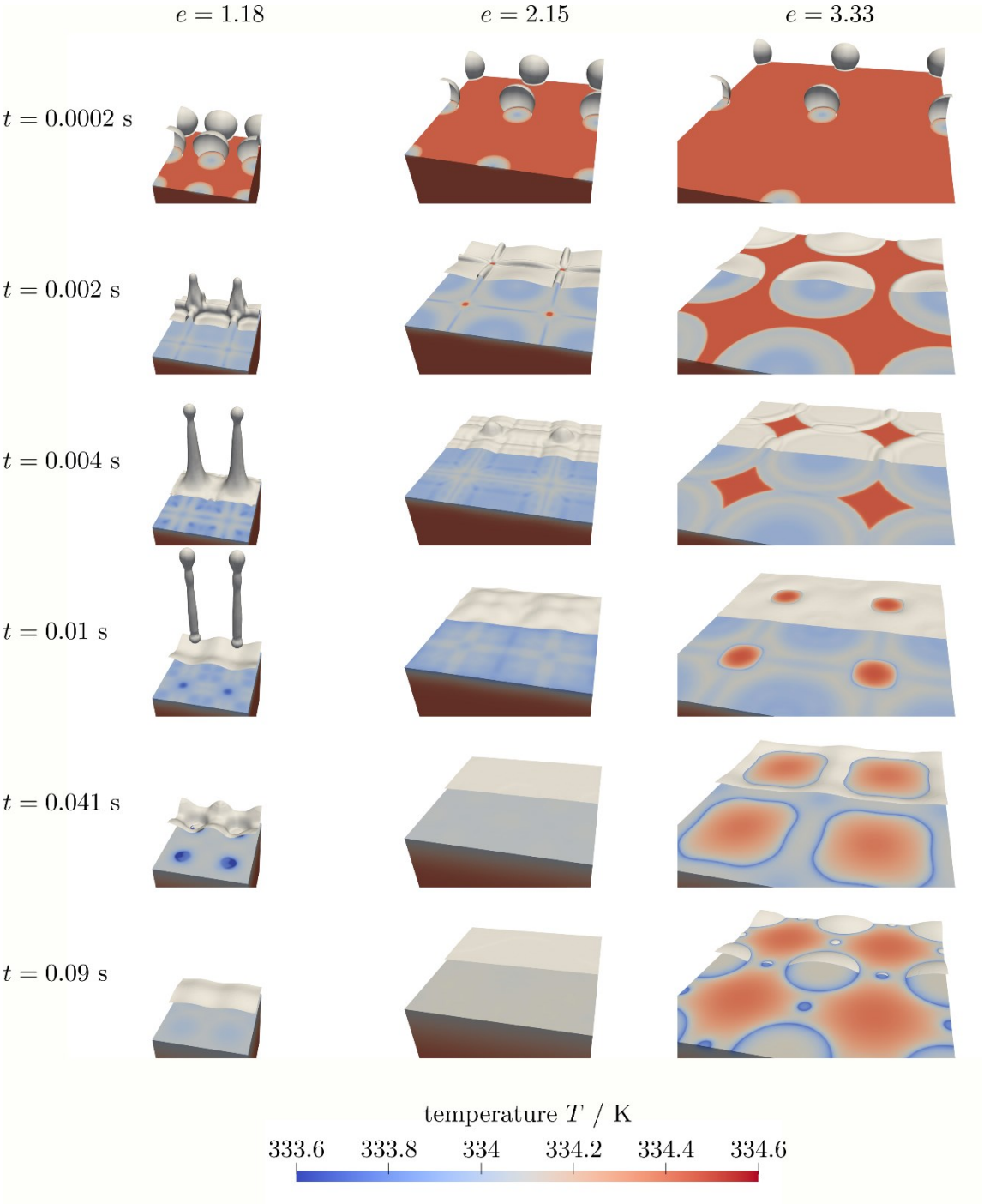

Figure 3 Temporal evolution of the wall temperature and the liquid-vapor interface for three different spacing parameters. The liquid-vapor interface is only visualized for the rear half of the presented section.

they start to coalesce. This results in a rapidly uprising liquid jet in the center between the drops (see $t = 0.002$ s). The uprising liquid jet forms a drop at its tip (see $t = 0.004$ s). Later, the jet fully separates from the liquid pool at the wall (see $t = 0.01$ s). This liquid jet falls back due to gravity and hits the liquid pool. This results in the formation of a liquid crater (see $t = 0.041$ s). Finally, a thin liquid pool is formed at the wall. We observe temperature minima at the wall in regions where the liquid swells up transporting cold liquid away from the wall. In addition, we observe temperature minima in regions where the liquid film is thin, e.g. as a result of the oscillating liquid pool and when the falling liquid jet hits the wall. The latter results

in a very pronounced temperature minimum as it has been also observed for multiple drop impingement onto a heated liquid pool [27].

For a larger spacing, i.e. $e = 2.15$, the drops coalesce at a later time compared to a smaller spacing. Consequently, the kinetic energy of the drops at the beginning of coalescence is lower. Hence, a small uprising liquid sheet forms at the intersection line of the drops (see $t = 0.002\ \mathrm{s}$) and a bump forms in the center between the drops (see $t = 0.004\ \mathrm{s}$). Just after that a liquid film covering the wall is formed. As in the case of the smaller spacing, we observe temperature minima in regions of the uprising liquid sheet and where the film is thin due to small oscillations.

In the case of a very large spacing, i.e. $e = 3.33$, only a small uprising liquid sheet forms at the intersection line of the drops (see $t = 0.004\ \mathrm{s}$). The liquid volume and kinetic energy of the drops are not large enough to cover the whole wall with a thin liquid film (see $t = 0.01\ \mathrm{s}$). Consequently, we observe a contact line, where there is significant heat transfer, resulting in rather low wall temperatures. Dry spots are characterized by high wall temperatures. This is not desirable for cooling applications. The liquid recedes (see $t = 0.041\ \mathrm{s}$) in order to achieve a circular drop shape. Finally, large and small sessile drops are observed at the wall (see $t = 0.09\ \mathrm{s}$).

For comparisons of our simulation results to the case of simultaneous impingement of two drops, we refer to similar experiments [14] and simulations [13,18]. Note that the simulations in [13,18] are performed under slightly different impact parameters as in the experiments [14]. Hence, we performed the simulations again with the same impact parameters as in the experiments [14]. The general fluid dynamics and heat transport behaviour are quantitatively still comparable to [13,18]. In agreement with the literature [16], we observe only for the smallest spacing the formation of the liquid jet in the case of the drop array impingement. We do not observe this liquid jet for the simultaneous impingement of two drops. In their work [16], the authors studied four spacing parameters ranging from $e = 1.3$ to $e = 2$.They also observe a liquid film completely covering the wall for the medium spacing ($e = 1.8$) and dry spots for the large spacing ($e = 2$). Moreover, they also observe dry spots at the wall for a low spacing ($e = 1.6$). This is, at least in part, qualitatively not in agreement with our results. Deviations could be due to a different range of impact parameters. The authors in [16] used a much higher Weber number ($We = 100$) and a much lower Reynolds number ($Re = 250$) than we do.

Figure 4 shows the temporal evolution of the wetted area. In the case of two simultaneously impinging drops, the wetted area increases, reaches a maximum and decreases to the wetted area covered by the combined sessile drop.

In contrast, the wetted area quickly reaches a constant value for the situation with small ($e = 1.18$) and medium ($e = 2.15$) spacing when the liquid pool forms. The final wetted area is lower, nearly equal, or higher for the drop array impingement compared to the simultaneous impingement of two drops for the small, medium, and large spacing, respectively.

In the case of the formation of a liquid film, a larger wetted area results in a higher heat flow. Although the wetted area of the drop array impingement is smaller for the large spacing ($e = 3.33$) than for the medium spacing ($e = 2.15$), the heat flow is higher for the large spacing. This shows the importance of the high heat flux at the contact line, which is absent if the liquid film covers the whole wall. For the small spacing ($e = 1.18$), the final heat flow, i.e. at time $t = 0.1\ \mathrm{s}$, is lower for drop array impingement compared to the case of two simultaneously impinging drops. For the large spacing ($e = 3.33$) this is vice versa.

To evaluate the total heat transferred, the temporal evolution of the cumulative heat flow is shown in Fig. 5. For the drop array impingement, the transferred heat increases with

increasing spacing. Only for the largest spacing ($e = 3.3$), the heat transfer is enhanced compared to two simultaneously impinging drops. This is due to the formation of multiple sessile drops, which are characterized by a thin liquid height (low thermal resistance) and a long contact line (strong evaporation). In the case of two simultaneously impinging drops, the dependence of cumulative heat flow on the spacing parameter is weaker than in the case of the drop array impingement.

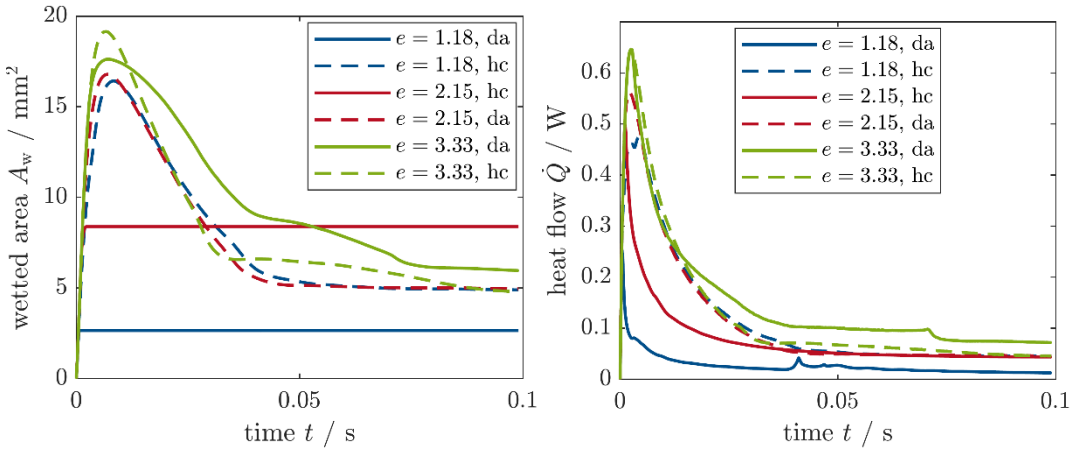

Figure 4 Temporal evolution of the wetted area (left) and the heat flow from the wall to the drop (right) for the drop array impingement ("da": drop array) and the simultaneous impingement of two drops ("hc": horizontal coalescence).

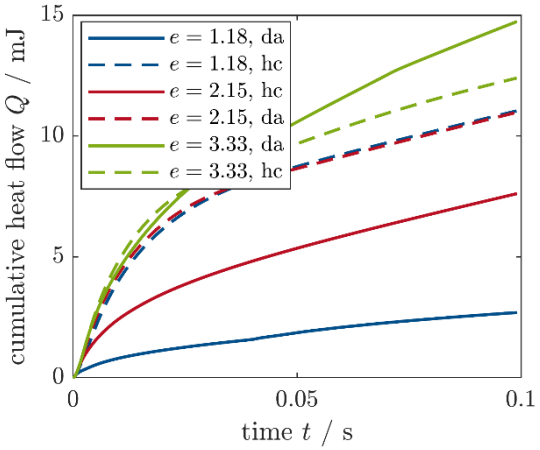

Figure 5 Temporal evolution of the cumulative heat flow from the wall to the drop for the drop array impingement (da, drop array) and the simultaneous impingement of two drops (hc, horizontal coalescence).

Note that in the case of the drop array impingement the above results are evaluated for the same liquid volume. Consequently, the smaller the spacing, the smaller the surface area of the wall under consideration. To take this into account, we also analyze the average heat flux. This shows us which configuration is more efficient in cooling the wall. In Fig. 6 we evaluate the average heat flux in two different ways. First, we divide the heat flow from the wall to the drop by the wetted area. One can see that a larger spacing results finally in a larger average heat flux. This means that small drops sitting on the wall are more efficient in cooling the wall than thin films. This is due to the strong evaporation at the contact line and the low average thermal resistance of the drop. The thinner film ($e = 2.15$) results in a higher heat flux

compared to the thicker film ($e = 1.18$). On the other hand, if we evaluate the heat flux by taking the total heat flow across the entire wall surface area and dividing it by the total wall surface area, the thin liquid films result in higher heat flux compared to the small drops. However, the final heat flux is almost identical in all three cases. On the one hand, small drops are more effective in cooling walls than thin films. On the other hand, the drops do not wet the entire wall resulting in dry spots with high wall temperatures and consequently a lower average heat flux is observed.

The local peak in the heat flux profiles for the small spacing ($e = 1.18$) at round about $t = 0.04$ s corresponds to the formation of the liquid crater resulting in low wall temperatures (see Fig. 2).

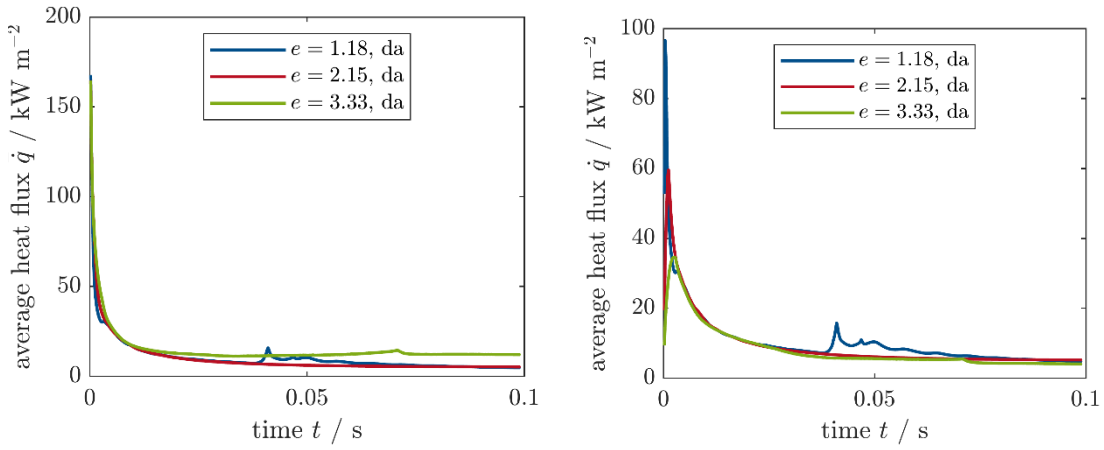

Figure 6 Temporal evolution of the average heat flux evaluated for the wetted area (left) and the total wall surface area (right) in the case of the drop array impingement (da, drop array).

Conclusions

We numerically investigated the simultaneous impingement of an array of drops onto a superheated wall for three different spacing parameters. We compared the results with the corresponding cases of two simultaneously impinging drops. We draw the following conclusions:

- For a small spacing, the impingement of an array of drops leads to the formation of an uprising liquid jet, while we do not observe these jets for the corresponding case of two simultaneously impinging drops. A small spacing results in the formation of a thin liquid film, while a large spacing results in small drops sitting on the wall.
- For the case of the impingement of an array of drops, the total heat transferred increases with increasing spacing. For a large spacing, the impingement of an array of drops transfers more heat than two simultaneously impinging drops, while for a small and medium spacing this is vice versa.
- Although small drops (large spacing) are more efficient at cooling the wall than thin liquid films (small and medium spacing), the thin liquid films cover the entire wall without dry spots, resulting in a slightly larger average total heat flux than the small drops.

Acknowledgement

We gratefully acknowledge the support from the Deutsche Forschungsgemeinschaft (DFG, German Research Foundation) within the Collaborative Research Center 1194 “Interaction between Transport and Wetting Processes” - Project-ID 265191195 - Subproject C02. We gratefully acknowledge the financial support from the Deutsche Forschungsgemeinschaft (DFG, German Research Foundation) - Priority Program “Dynamic Wetting of Flexible, Adaptive and Switchable Surfaces” (SPP 2171), Project number 422792679. We gratefully acknowledge the support from the Deutsche Forschungsgemeinschaft (DFG, German Research Foundation) - Project SFB-TRR 75, Project number 84292822. This article was written as part of the LoTuS project (funding code 03EN2026), which is funded by the Bundesministerium für Wirtschaft und Klimaschutz (BMWi, German Federal Ministry for Economic Affairs and Climate Protection) and supervised by the project executing organization Jülich. Calculations for this research were conducted on the Lichtenberg high-performance computer at the Technical University of Darmstadt.

Nomenclature

Symbol	Unit	Description
$c_{p,s}$	$\mathrm{J\,kg^{-1}\,K^{-1}}$	Specific heat capacity
D	m	Diameter
d	m	Distance
e	-	Spacing factor
$\boldsymbol{f}_g, \boldsymbol{f}_\sigma$	$\mathrm{N\,m^{-3}}$	Momentum source term
h	$\mathrm{J\,kg^{-1}}$	Enthalpy
p_{rgh}	bar	Pressure
$\dot{q}_{\mathrm{pc}}$	$\mathrm{W\,m^{-3}}$	Energy source term
T	K	Temperature
ΔT	K	Wall superheat
u	$\mathrm{m\,s^{-1}}$	Velocity
α	-	Volume fraction
$\dot{\alpha}_{\mathrm{pc}}$	$\mathrm{kg\,s^{-1}m^{-3}}$	Mass source term
λ	$\mathrm{W\,m^{-1}\,K^{-1}}$	Thermal conductivity
μ	$\mathrm{kg\,m^{-1}\,s^{-1}}$	Dynamic viscosity
ρ	$\mathrm{kg\,m^{-3}}$	Density

References

[1] J. Kim. Spray cooling heat transfer: The state of the art. International Journal of Heat and Fluid Flow 28: 753-767 (2007).

[2] G. Liang and I. Mudawar. Review of spray cooling – part 1: Single-phase and nucleate boiling regimes, and critical heat flux. International Journal of Heat and Mass Transfer 115: 1174-1205 (2017).

[3] G. Liang and I. Mudawar. Review of spray cooling – part 2: High temperature boiling regimes and quenching applications. International Journal of Heat and Mass Transfer 115: 1206-1222 (2017). 4-1205 (2017).

[4] J. Duarte Benther, J. Pelaez-Restrepo, C. Stanley, and G. Rosengarten. Heat transfer during multiple droplet impingement and spray cooling: Review and prospects for enhanced surfaces. International Journal of Heat and Mass Transfer 178: 121587 (2021).

[5] G. Liang and I. Mudawar. Review of drop impact on heated walls. International Journal of Heat and Mass Transfer 106: 103-126 (2017).

[6] A. Yarin. Splashing, spreading, receding, bouncing…Annual Review of Fluid Mechanics 38: 159: 126 (2006).
[7] M. Marengo, C. Antonini, I. V. Roisman, and C. Tropea. Drop collisions with simple and complex surfaces. Current Opinion in Colloid & Interface Science 16: 292-302 (2011).
[8] C. Josserand and S. T. Thoroddsen. Drop impact on a solid surface. Annual Review of Fluid Mechanics 16: 365-391 (2016).
[9] J. Breitenbach, I. V. Roisman, and C. Tropea. "From drop impact physics to spray cooling models: a critical review. Experiments in Fluids 59: 55 (2018)
[10] M. Rein. Phenomena of liquid drop impact on solid and liquid surfaces. Fluid Dynamics Research 12: 61-93 (1993).
[11] I.V. Roisman, B. Prunet-Foch, C. Tropea, M. Vignes-Adler. Multiple Drop Impact onto a Dry Solid Substrate. Journal of Colloid and Interface Science 256: 396-410 (2002).
[12] N. Ersoy, M. Eslamian. Central uprising sheet in simultaneous and near-simultaneous impact of two high kinetic energy droplets onto dry surface and thin liquid film. Physics of Fluids 32: 012108 (2020).
[13] S. Batzdorf, J. Breitenbach, C. Schlawitschek, I.V. Roisman, C. Tropea, P. Stephan, T. Gambaryan-Roisman. Heat transfer during simultaneous impact of two drops onto a hot solid substrate. International Journal of Heat and Mass Transfer 113: 898-907 (2017).
[14] A. Gholijani, T. Gambaryan-Roisman, P. Stephan. Experimental investigation of hydrodynamics and heat transport during horizontal coalescence of two drops impinging a hot wall. Experimental Thermal and Fluid Science 131: 110520 (2022).
[15] A. Gultekin, N. Erkan, E. Ozdemir, U. Colak, S. Suzuki. Lattice Simultaneous multiple droplet impact and their interactions on a heated surface. Experimental Thermal and Fluid Science 120: 110255 (2021).
[16] W. Zhou, D. Loney, A. Fedorov, F. Degertekin, D. Rosen. Lattice Boltzmann simulations of multiple-droplet interaction dynamics. Physical Review E 89: 033311 (2014).
[17] J. Duarte Benther, V. Bhatt, J. Pelaez Restrepo, C. Stanley, G. Rosengarten. Non-simultaneous droplet impingement cooling of a solid heated surface. International Journal of Heat and Mass Transfer 191: 122752 (2022).
[18] S. Batzdorf. Phenomena of liquid drop impact on solid and liquid surfaces. Dissertation, TU Darmstadt, http://tubiblio.ulb.tu-darmstadt.de/73268/, (2015).
[19] TwoPhaseFlow. https://github.com/DLR-RY/TwoPhaseFlow (2019).
[20] H. Scheufler, J. Roenby. TwoPhaseFlow: A Framework for Developing Two Phase Flow Solvers in OpenFOAM. OpenFOAM Journal 3: 200-224 (2023).
[21] H. Scheufler, J. Roenby. Accurate and efficient surface reconstruction from volume fraction data on general meshes. Journal of Computational Physics 383: 1-23 (2019).
[22] J. Roenby, H. Bredmose, H. Jasak. A computational method for sharp interface advection. Royal Society Open Science 3: 160405 (2016).
[23] S. Hardt, F. Wondra. Evaporation model for interfacial flows based on a continuum-field representation of the source terms. Journal of Computational Physics 227: 5871-5895 (2008).
[24] P. Stephan, C.A. Busse. Analysis of the heat transfer coefficient of grooved heat pipe evaporator walls. International Journal of Heat and Mass Transfer 35: 383-391 (1992).
[25] C. Schlawitschek. Numerical simulation of drop impact and evaporation on superheated surfaces at low and high ambient pressures. Dissertation, TU Darmstadt, http://tuprints.ulb.tu-darmstadt.de/11800/, (2020).
[26] H. Sontheimer, A. Gholijani, P. Stephan, T. Gambaryan-Roisman. Hydrodynamics and heat transport during the vertical coalescence of multiple drops impacting successively onto a hot wall. International Journal of Heat and Mass Transfer 204: 123856 (2023).
[27] G. Liang, T. Zhang, L. Chen, Y. Chen, S. Shen. Single-phase heat transfer of multi-droplet impact on liquid film. International Journal of Heat and Mass Transfer 132: 288-292 (2019).